Chemical Engineering Journal 376 (2019): 120431

DOI: https://doi.org/10.1016/j.cej.2018.11.129

Catalytic wet peroxide oxidation of imidazolium-based ionic liquids: catalyst stability and biodegradability enhancement

Ismael F. Mena,[a*] Elena Diaz,[a] Citlali Pérez-Farías,[b] Stefan Stolte,[c] Ivan Moreno-Andrade,[b] Juan J. Rodriguez,[a] Angel F. Mohedano[a]

[a]Chemical Engineering Section, Universidad Autónoma de Madrid, Campus de Cantoblanco, 28049 Madrid, Spain.

[b] Laboratorio de Investigación en Procesos Avanzados de Tratamiento de Aguas, Unidad Académica Juriquilla–Querétaro, Instituto de Ingeniería, Universidad Nacional Autónoma de México, México.

[c] Institute of Water Chemistry, Department of Hydrosciences, Technische Universität Dresden, Bergstraße 66, 01069 Dresden, Germany

[*]Corresponding author. Tel.: +34 914 973525; Fax: +34 914 973516

E-mail address: ismael.fernandez@uam.es

Abstract

The catalytic wet peroxide oxidation (CWPO) of the imidazolium-based ionic liquids 1-butyl-3-methylimidazolium chloride (BmimCl), 1-butyl-3-methylimidazolium acetate (BmimAc), 1-butyl-3-methylimidazolium *bis*(trifluoromethanesulfonyl)imide ($BmimNTf_2$), 1-hexyl-3-methylimidazolium chloride (HmimCl) and 1-decyl-3-methylimidazolium chloride (DmimCl) was examined by using a Fe catalyst supported on alumina (Fe_2O_3/Al_2O_3) that was prepared by incipient wetness impregnation. Variable H_2O_2 doses from 0.5 to 1.5 times the stoichiometric value provided similar results in terms mg TOC removed per mg H_2O_2 decomposed at 80 ºC (0.033 mg_{TOC} mg_{H2O2}^{-1}), all allowing complete $Bmim^+$ removal. Raising the reaction temperature to 90 ºC increased the mineralization rate up to 40 % TOC conversion. Differences in TOC conversion among counteranions (chloride, acetate and NTf_2^-) were negligible. A plausible reaction pathway is propose involving hydroxylated compounds and short-chain organic acids as reaction byproducts. CWPO markedly increased the subsequent biodegradability of the IL test solutions and led there to TOC conversions after CWPO-biodegradability assays of 55–60 %. The Fe_2O_3/Al_2O_3 catalyst exhibited high long-term stability; thus, it retained most of its properties and underwent negligible Fe leaching.

Keywords: Imidazolium, Heterogeneous Fenton, Ionic liquids, Sewage sludge, Toxicity, Biodegradability

1. Introduction

Ionic Liquids (ILs) are salts with melting points below 100 ºC formed by an organic cation and an organic or inorganic anion of widely variable nature. ILs can possess a low vapor pressure, good chemical and physical stability, and a high solubility in water, all of which have aroused much attention with a view to their industrial application in green chemistry [1–3]. However, ILs are not necessarily "green" solvents, even though they are less polluting than the typical volatile organic solvents. In fact, the toxic nature and low biodegradability in water of cetain ILs may raise environmental concerns arising from their persistence in water [4–7] and polluting potential [8–10].

The imidazolium family of ILs is probably the most extensively studied on account of their wide use as solvents in major chemical (catalysis, biocatalysis, synthesis) and electrochemical processes. As a result, these compounds, which essentially consist of an aromatic heterocycle containing two nitrogen atoms —one in cationic form—, can reach industrial wastewater through production processes and use [11]. Some studies have examined the ecotoxicity and biodegradability of imidazolium ILs to assess their potential hazards for the aquatic environment [4–6,12–15]. The ecotoxicity of wastewater or inhibitory compounds in aquatic environments is typically assessed with microorganisms such as bacteria or algae, or fish [7,15,16]. Overall, the ecotoxicity of imidazolium-based ILs depends on the particular cation and anion. As far as the cation is concerned, ecotoxicity increases with increasing length of the alkyl chain [7,17]; for example, EC_{50} values, the concentration of a pollutant that reduces microbial activity by 50 %, against *Vibrio fischeri* have been found to increase from 8.12 mM with a chain of 4 carbon atoms to 12.3 μM with one of 10. Ionic liquids such as BmimCl [4] or Bmim ethyl sulfate [15] have EC_{50} values similar to those for conventional organic solvents such as dichloromethane or chloroform [18]. However, BmimBr shows much lower

effective concentration than conventional solvents (e.g., 700 times more than methanol against *Selenastrum capricornutum* [12]). Also, fluorine-containing anions such as bitriflimide and tetrafluoroborate are more ecotoxic for *Vibrio fischeri* than other anion moieties [19].

Biodegradability in imidazolium ILs is seemingly related to the length of the alkyl side chain. By using a modified OECD Guideline (OECD 1992), Docherty et al. [20] showed that, although HmimBr and OmimBr ILs are classified as non-readily biodegradable, they can be partially mineralized by an activated sludge microbial community incubated for 25 h. Thus, they obtained a TOC conversion of 54 and 41 % for HmimBr and OmimBr, respectively, but found the concentration of BmimBr to remain unchanged; therefore, a longer alkyl side chain resulted in faster degradation rates. On the other hand, Stolte et al. [21] used a modified version of OECD guideline 301 D to measure IL cation concentrations by HPLC–UV. They observed primary biodegradation of activated sludge (5 g L^{-1}) with HmimCl and OmimCl (viz., 11 and 100 % of removal, respectively, after 21 days), but no degradation with BmimCl. The proposed biodegradation pathway for these imidazolium-based ILs includes transformation of the alkyl chain but no change in the imidazolium ring [9,21].

Based on the foregoing, it is essential to know whether destructive technologies such as advanced oxidation processes (AOPs), which have so far provided excellent results in removing refractory or nonbiodegradable pollutants from wastewater streams, are also efficient in detoxifying IL-polluted effluents [22,23]. Scarce research has to date been conducted on the degradation of imidazolium ILs by AOPs. In one study, boron-doped diamond electrodes were used to analyze the electrochemical oxidation of imidazolium ILs for the influence of the anions in Bmim-based ILs; degradation was fastest with BmimCl and slowest in the presence of an aromatic anion ($CH_3C_6H_4SO_3$) [24].

Siedlecka et al. (2012) studied the influence of the cation on the electrochemical oxidation of BmimCl and OmimCl with a PbO_2 anode and found their degradation rate to be quite similar and slightly higher than that of Omim [25]. COD removal with BmimCl and OmimCl was 80 and 75 %, respectively, and nitrogen conversion to ammonium and nitrate ions 80 and 60 %, respectively. Pieczynska et al. [26] examined the influence of temperature and pH, and found it to be negligible in BmimCl electrochemical oxidation; also, they proposed a reaction pathway for imidazolium-based ILs involving carboxylic acids of low molecular weight, CO_2, H_2O, NH_4^+ and NO_3^- as end products. Garcia-Segura et al. [27] studied various electroprocesses for the abatement of 1-Ethyl-3-metylimidazolium chloride (EmimCl) by degradation and found electro-Fenton and photoelectron-Fenton to boost degradation of the cation and mineralization (TOC conversions were close to 80 % in all cases). Recent studies of bare-electrolysis, photoelectrolysis, sonoelectrolysis and electrolysis in presence of sulfates anions reveals that the NTf_2^- anion is recalcitrant to electroxidation processes, although are effectives in the degradation of the imidazolium cations, with TOC conversions near 90% in the BmimCl electrolysis with sulfates anions [28–30]. Ultraviolet photolysis, photolysis plus hydrogen peroxide (UV/H_2O_2) and photocatalysis with TiO_2 at room temperature for the removal of BmimCl, HmimCl and OmimCl revealed that the extent of degradation decreased with increasing size of the alkyl side chain and was 60, 85 and 95 %, respectively [31]. Czerwicka et al. [32] studied the degradation of the imidazolium chloride family of ILs with H_2O_2/UV and found the process to involve a large number of intermediate degradation products. A recent study revealed an increased ecotoxicity of such intermediates to *Daphnia magna* and *Raphidocelis subcapitata* in the UV/H_2O_2 effluent [33]. As can be seen, Siedlecka et al. (2008 and 2009) studied the Fenton reaction of Bmim-based ILs at a 1 mM

concentration allowed complete degradation of the cations within 150 min; the outcome was strongly influenced by the IL anion, BmimCl being the least easily degraded IL and $BmimCF_3SO_3$ the most [34,35]. Munoz et al. (2015a,b) studied the influence of the reaction temperature by using a 1 g L^{-1} concentration of EmimCl, 50 mg L^{-1} Fe^{3+} and the stoichiometric amount of H_2O_2; raising the temperature from room level to 50–90 ºC ensured complete degradation within 5 min and mineralization rates of 30–50 % in all cases [36,37]. Catalytic wet peroxide oxidation (CWPO), which involves the formation of HO· radicals by catalytic decomposition of H_2O_2 in an acid medium containing a supported Fe catalyst [38], has been successfully used to degrade imidazolium-based ILs. Thus, Munoz et al. [39] examined the degradation of EmimCl, BmimCl and OmimCl (1 g L^{-1}) with three different catalysts (Fe_3O_4/Al_2O_3, Fe_3O_4/AC Graphite) by using a stoichiometric amount of H_2O_2 at 90 ºC at pH 3. These conditions allowed complete removal of EmimCl within 5 min and provided mineralization rates around 40-50 %. The degradation rate was only slightly influenced by the length of the alkyl chain. Poza-Nogueira et al. [40] studied the heterogeneous electro-Fenton using iron alginate spheres of 1,3-Bis(2,4,6-trimethylphenyl)imidazolinium chloride achieved a 77% of TOC abatement in 2 h of treatment.

Table 1 summarizes the main results reported in the literature about the abatement of imidazolium ILs by Fenton and CWPO oxidation.

Table 1. Summary on the application of Fenton and CWPO oxidation to imidazolium-based ILs.

IL	Process	Operating conditions	IL removal (%/time)	TOC conversion (%/time)	Reference
1-Butyl-3-methylimidazolium chloride	Fenton	[IL] = 1 mM, [Fe^{2+}] = 0.5-1.5 mM, [H_2O_2] = 10-400 mM, T = 25 ºC, pH_0: 3-4	100/150 min	-	Siedlecka et al. 2008 [34]
1-Butyl-3-methylimidazolium chloride 1-Butyl-3-methylimidazolium trifluoromethanesulfonate 1-Butyl-3-methylimidazolium tricyanmethide	Fenton	[IL] = 1 mM, [Fe^{2+}] = 1 mM, [H_2O_2] = 100 mM, T = 25 ºC, pH_0: 3	100/45-150 min	-	Siedlecka et al. 2009 [35]
1-Ethyl-3-methylimidazolium chloride 1-Butyl-3-methylimidazolium chloride 1-Methyl-3-octylimidazolium chloride 1-Dodecyl-3-methylimidazolium chloride 1-Methyl-3-tetradecyl imidazolium chloride 1-Hexadecyl-3-methylimidazolium chloride 1-Butyl-3-methylimidazolium methanesulfonate 1-Butyl-3-methylimidazolium methylsulfate 1-Butyl-3-methylimidazolium acetate	Fenton	[IL] = 1000 mg L^{-1}, [Fe^{3+}] = 50 mg L^{-1}, [H_2O_2] = stoichiometric dose, T = 50-90 ºC, pH_0: 3	85-100/10-240 min	10-65/240 min	Dominguez et al. 2014 [41]
1-Ethyl-3-methylimidazolium chloride	Fenton	[IL] = 1000 mg L^{-1}, [Fe^{3+}] = 10-125 mg L^{-1}, [H_2O_2] = stoichiometric dose, T = 50-90 ºC, pH_0: 3	100/<10 min	18-56/240 min	Munoz et al. 2015 a [37]
1-Ethyl-3-methylimidazolium chloride 1-Butyl-4-methylpyridinium chloride 1-Ethyl-3-methylimidazolium tetracyanoborate 1-Ethyl-3-methylimidazolium dicyanamide 1-Ethyl-3-methylimidazolium tricyanomethanide 1-Ethyl-3-methylimidazolium thiocyanate 1-Ethyl-3-methylimidazolium dimethylphosphate	Fenton	[IL] = 1000 mg L^{-1}, [Fe^{3+}] = 50 mg L^{-1}, [H_2O_2] = stoichiometric dose, T = 70 ºC, pH_0: 3	-	44-80/240 min	Munoz et al. 2015 b [36]

1-Ethyl-3-methylimidazolium tosylate					
1-Ethyl-3-methylimidazolium hexafluorophosphate	Fenton	[IL] = 0.5-10 mM, [Fe^{2+}] = 0.5-5 mM, [H_2O_2] = 5-50 mM, T = 25-70 ºC, pH_0: 3-11	28-96/120 min	<52/120 min	Cheng et al. 2016 [42]
1-Butyl-3-methylimidazolium chloride	Fenton	[IL] = 100-1000 mg L^{-1}, [Fe^{3+}] = 10-50 mg L^{-1}, [H_2O_2] = 50-200 % stoichiometric doses, T = 50-90 ºC, pH_0: 3	100/1.5-5 min	-	Dominguez et al. 2017 [43]
1-Hexyl-3-methylimidazolium chloride	Fenton	[IL] = 1000 mg L^{-1}, [Fe^{3+}]/[H_2O_2] = 1/10 (M/M), [H_2O_2] = 20-100 % stoichiometric doses, T = 70 ºC, pH_0: 3	58-100/240 min	6-53/240 min	Gomez-Herrero et al. 2018 [44]
1-Ethyl-3-methylimidazolium chloride 1-Butyl-3-methylimidazolium chloride 1-Methyl-3-octylimidazolium chloride 1-Hexadecyl-3-methylimidazolium chloride	CWPO	[IL] = 1000 mg L^{-1}, [Fe_3O_4/γ-Al_2O_3] = 2 g L^{-1}, [H_2O_2] = stoichiometric dose, T = 90 ºC, pH_0: 3	100/30-60 min	33-44/240 min	Munoz et al. 2016 [39]
		[IL] = 1000 mg L^{-1}, [Fe_3O_4/AC] = 2 g L^{-1}, [H_2O_2] = stoichiometric dose, T = 90 ºC, pH_0: 3	100/30 min	43/240 min	
		[IL] = 1000 mg L^{-1}, [Graphite] = 2 g L^{-1}, [H_2O_2] = stoichiometric dose, T = 90 ºC, pH_0: 3	100/30 min	36-53/240 min	
1-Hexyl-3-methylimidazolium dicyanamide 1-Butyl-3-methylimidazolium dicyanamide 1-Ethyl-3-methylimidazolium dicyanamide 1-Ethyl-3-methylimidazolium acetate	Heterogeneous electro-Fenton	[IL] = 0.5 g L^{-1}, current = 100-300 mA, [iron alginate spheres] = 3.2-5.33 g L^{-1}, pH_0: 3	80-100/120 min	40-100/120 min	Bocos et al. 2017 [45]

1-Ethyl-3-methylimidazolium methylsulfate					
1,3-Bis(2,4,6-trimethylphenyl)imidazolinium chloride	Heterogeneous electro-Fenton	[IL] = 0.2-0.8 mM, current = 50-300 mA, [iron alginate spheres] = 1-5 g L^{-1}, pH_0: 3	-	36-77/120 min	Pazo-Nogueira et al. 2018 [40]

*Imidazolium cation conversion

The main aim of this work was to assess the efficiency of CWPO with an Fe_2O_3/Al_2O_3 catalyst to detoxify synthetic wastewater polluted with imidazolium ILs (BmimCl, BmimAc, $BmimNTf_2$, HmimCl and DmimCl) focusing on the influence of the operating conditions (temperature and H_2O_2 dose) and IL structure (nature of the anion and length of the alkyl chain), including a possible reaction pathway for the $Bmim^+$ imidazolium cation. The biodegradability enhancement and the acute toxicity (towards *Daphnia magna*) of the effluents have been also evaluated. Finally, the stability of the catalyst is studied in long-term continuous experiments, including the catalyst characterization before and after the CWPO reactions.

2. Material and methods

2.1. Ionic liquids

The ILs studied, which included 1-butyl-3-methylimidazolium chloride (BmimCl, > 98 % purity), 1-butyl-3-methylimidazolium acetate (BmimAc, > 95 % purity), 1-butyl-3-methylimidazolium *bis*(trifluoromethanesulfonyl)imide ($BmimNTf_2$, > 99 % purity), 1-hexyl-3-methylimidazolium chloride (HmimCl, > 97 % purity) and 1-decyl-3-methylimidazolium chloride (DmimCl, > 96 % purity), were purchased from either Iolitec or Sigma–Aldrich. Table 1S shows the structure of the cations and anions selected in this study.

2.2. Preparation and characterization of the Fe_2O_3/Al_2O_3 catalyst

The Fe_2O_3/Al_2O_3 catalyst was prepared by incipient wetness impregnation of Al_2O_3 supplied by Merck (Germany), using an aqueous solution of $Fe(NO_3)_3 \cdot 9H_2O$ to obtain a nominal 4 % (w/w) concentration. Once impregnated, the solid was dried at 60 ºC for 12 h and calcined for 4 h at 300 ºC, which was reached at 3 ºC min^{-1} [46].

The catalyst was characterized as follows before and after use in the CWPO reaction. Nitrogen adsorption–desorption isotherms at 77 K were obtained by using a Micromeritics Tristar 3020 automated volumetric gas adsorption instrument. The samples (0.15 g) were degasified at 150 ºC for 7 h in a Micromeritics VacPrep 061 degassing system under vacuum to determine their BET area and total volume of mesopores. The iron content of the catalyst was determined by total reflection X-ray fluorescence (TXRF) spectroscopy, using a TXRF Extra-II Rich & Seifert spectrometer equipped with an Si–Li detector. C, H, N and S were quantified with a LECO CHNS-932 elemental analyzer. The composition and the Fe species of the catalyst surface was determined by X-ray photoelectron spectroscopy (XPS) on a Physical Electronics 5700C Multitechnique instrument from Physical Electronics using MgKa radiation (1253.6 eV) in combination with energy dispersive X-ray spectroscopy analysis (EDAX). The morphology and surface composition of the catalyst were analyzed by Scanning Electron Microscopy–Energy Dispersive X- ray spectroscopy (SEM-EDX) with a Hitachi S-3000N apparatus. The crystalline phases in the catalysts were analyzed by X-ray diffraction (XRD) using a Siemens model D-5000 diffractometer with Cu Kα radiation.

Table 2 collects the main characteristics of the fresh Fe_2O_3/Al_2O_3 catalyst. A total Fe content of 3.9 % w/w is uniformly distributed on the catalyst surface as evidence the Fe_{TXRF}/Fe_{XPS} ratio and the SEM analysis (Figure 1S). The XPS spectrum of the Fe 2p region (Figure 2S) presents a main band centered at 711.4 eV, accompanied by a secondary one at 725.1 eV, and a satellite peak around 719.0 eV associated to the presence of Fe^{3+} species in the catalyst surface, as has been previously reported [47,48]. XRD analysis indicated that the catalyst presents two crystalline phases, γ-Al_2O_3 and

hematite, α-Fe_2O_3 (Figure 3S). The N_2 adsorption-desorption isotherm corresponds with a mainly mesoporous material (Figure 4S).

Table 2. Representative characterization of the fresh and used Fe_2O_3/Al_2O_3 catalyst in a long-term experiment at 80 h ([BmimAc] = 1 mM, $[H_2O_2]$ = 27 mM, pH_0 = 3, τ = 3.33 $kg_{Fe2O3/Al2O3}$ h mol_{IL}^{-1}).

Fe_2O_3/Al_2O_3 Catalyst	Fresh	Used
Fe_{TXRF} (w/w %)	3.90	3.86
Fe_{XPS} (w/w %)	4.60	4.56
Fe_{TXRF}/Fe_{XPS}	0.85	0.86
BET area (m^{-2} g^{-1})	131	120
$V_{mesopore}$ (cm^3 g^{-1})	0.134	0.110

2.3. CWPO experiments

CWPO runs were conducted in duplicate at atmospheric pressure in a 400 mL glass batch reactor equipped with a magnetic stirrer (500 rpm) and temperature control. The starting concentration of IL was 1 mM, the catalyst concentration 1000 mg L^{-1} (40 mg Fe L^{-1}), and the initial pH 3. The variables studied were $[H_2O_2]_0$ (0.5–1.5 times the stoichiometric doses, which was the theoretical amount of H_2O_2 needed for complete mineralization to CO_2, H_2O and N_2 of the starting compound) and reaction temperature (70–90 ºC). Blank runs in the absence of catalyst were also carried out at all temperatures and negligible conversions of all ILs (< 3%) invariably obtained in them. The process was monitored by periodically analyzing samples from the batchwise runs. A Fenton run was also performed in parallel for comparison with CWPO by using the same Fe concentration (40 mg L^{-1}, provided by $FeCl_3 \cdot 6H_2O$ salt), 1 mM BmimCl, the stoichiometric amount of H_2O_2, pH 3 and 80 ºC. Long-term runs (80 h on stream) were performed in a continuous stirred batch reactor (CSTR) fitted with a Gilson FC 203B autosampler to collect reaction aliquots. The ionic liquids and H_2O_2 were fed to the

reactor at a 1 mL min^{-1} flow rate in order to deliver an IL concentration of 1 mM and the stoichiometric H_2O_2 dose for a space–time of 3.33 $kg_{Fe2O3/Al2O3}$ h mol_{IL}^{-1}. IL concentrations were determined on a Varian Prostar 325 high performance liquid chromatograph equipped with an UV–Vis detector operated at 218 nm and furnished with a Synergy 4 mm Phenomenex Polar-RP 80 A column 15 cm long × 4.6 mm i.d. as stationary phase. The mobile phase, run at 0.75 mL min^{-1}, was a mixture of phosphate buffer and acetonitrile at different concentrations from 5 to 40 % v/v depending on the particular imidazolium cation. Short-chain organic acids (formic, acetic, malonic and oxalic) and anionic species (chloride and nitrate) were determined on a DIONEX ICS-900 ion chromatograph with chemical suppression furnished with a Dionex IonPac AS22 4 × 250 mm column and using 1.4 mM $NaHCO_3$/4.5 mM Na_2CO_3 at 1 mL min^{-1} as mobile phase. TOC was measured with a Shimadzu TOC-VCSH TOC analyzer, and H_2O_2 by colorimetric titration on a Cary 60 UV/Vis spectrophotometer from Agilent that was used at 410 nm to monitor the formation of the Ti(IV)–H_2O_2 complex [49]. Iron leached from the catalyst to the liquid phase was measured by colorimetric titration at 510 nm (the *o*-phenanthroline method) [50]. NTf_2^- anion was identified by liquid chromatography coupled with mass spectrometry (LC/MS SQ Agilent), using an ACE Excel 3 C18-Amide 150 × 4.6 mm column at 40 ºC as stationary phase and a 10:90 v/v mixture of formic acid and acetonitrile at 0.2 cm^3 min^{-1} as mobile phase. This instrument was also used for the tentative identification of reaction byproducts; by exception, the mobile phase was a 99.9:0.1 v/v mixture of water and formic acid, and its flow rate 0.5 mL min^{-1}. Mass spectra were acquired over the *m*/*z* range 40–400.

The initial IL solutions and CWPO reaction effluents were assessed for biodegradability in terms of toxicant removal efficiency, which was in turn measured in terms of IL and TOC concentrations, and of microbial activity [51–53]. For this purpose, a closed

reactor was loaded with unacclimated sludge (350 mg L^{-1}) and the target compound. The specific oxygen uptake rate (SOUR) profile was measured interrupting the air supply and registering the dissolved oxygen decay within a range of 0.1 mg L^{-1}, obtaining the oxygen uptake rate (OUR) as the slope of the oxygen concentration vs time plot, and relating it to the biomass concentration added in the reactor. All runs were carried out at 25 ºC for 100 h.

Daphtoxkit F (MicroBioTest Inc., Gent, Belgium) was used for 48 h to conduct an acute immobilization test with *Daphnia magna* according to ISO 6341. Solution concentrations were adjusted to the particular IL, namely: 5–250 mM for BmimCl, BmimAc and $BmimNTf_2$; 1–50 mM for HmimCl and 0.05–20 mM for DmimCl. All runs were done in duplicate, using four replicates of each concentration in 10 mL of mineral medium (controls) or solution of test substances in mineral medium. Each replicate involved using five pre-fed *Daphnia* neonates that were less than 90 h old and obtained at 20 °C under continuous lighting. Sample toxicity was assessed from the number of immobilized or dead organisms after 24 and 48 h as a fraction of unaffected organisms compared to the controls.

3. Results and discussion

3.1. CWPO of Bmim-based ILs

Preliminary runs were used to assess the degradation of the model IL BmimCl under identical conditions in the Fenton and CWPO reaction. As can be seen from Figure 1, $Bmim^+$ was degraded more rapidly in the homogeneous reaction (complete removal took only 30 min) than by CWPO, which took more than 60 min. The pH value slightly decreased from 3.0 to 2.8, due to the formation of carboxylic acids as final reaction products. The initial reaction rate for $Bmim^+$ disappearance was estimated to be $4.1 \cdot 10^{-1}$

min^{-1} and $5.2 \cdot 10^{-2}$ min^{-1} for Fenton and CWPO, respetively. The difference can be ascribed to the fact that the hydrogen peroxide uptake was initially (first 15 min) three times higher with Fenton but then changed similarly in both reactions and approached 80 % after 240 min. As shown by the increased mineralization achieved relative to CWPO, BmimCl was more efficiently oxidized by the Fenton reagent. Fe leaching during the CWPO reaction was less than 0.04 mg L^{-1} and similar to previous results for alumina-supported Fe catalysts in other CWPO reactions [46,54]. Therefore, any contribution of the homogeneous reaction to the CWPO process must have been negligible.

The influence of the H_2O_2 concentration, the highest cost related to the CWPO process, on the CWPO reaction of BmimCl was studied by using variable H_2O_2 doses from 0.5 to 1.5 times the stoichiometric value (12–36 mM) at 80 ºC ($[IL]_0$ = 1 mM, $[Fe_2O_3/Al_2O_3]_0$ = 1g L^{-1}, pH 3, 240 min). Based on the results, the lowest H_2O_2 dose led to the lowest $Bmim^+$ degradation. However, no significant differences in $Bmim^+$ reaction rate were observed with an amount of H_2O_2 equivalent to 1 or 1.5 times the H_2O_2 stoichiometric concentration. H_2O_2 conversion during the CWPO reaction evolved identically with 0.5 and 1.0 times the H_2O_2 stoichiometric doses, but was slightly higher with the highest dose (1.5 times the stoichiometric amount). Despite of TOC conversion at the end of the reaction ranged from 11 and 34 %, which was proportional to the initial H_2O_2 concentration, but a H_2O_2 dose superior to 2 times of stoichiometric did not cause the same increment (data not shown). The Fe leaching increased when the H_2O_2 dose increased (Figure 2b), but in all cases these value are below 0.05 mg L^{-1}. The H_2O_2 uptake efficiency as measured through the amount of TOC removed per unit H_2O_2 decomposed was 0.033 mg_{TOC} mg_{H2O2}^{-1} in the range of the initial H_2O_2 concentrations studied. This value is 3.4 times lower than that previously obtained in the degradation of

phenol with a $\gamma Fe_2O_3/Al_2O_3$ catalyst [46] and bisphenol A with a Fe-carbon support obtained from grape seeds [53]. Figure 3 shows the evolution of short-chain acids (formic, acetic, malonic and oxalic) during the CWPO reaction. The rates of formation and disappearance of formic and malonic acid increased with increasing H_2O_2 dose. On the other hand, the concentrations of acetic and oxalic acid, which have been deemed refractory to CWPO, increased with increasing dose. Although no nitrite anion was detected in the reaction medium, a concentration of 0.06 mM of nitrate anion was quantified due to the degradation of the imidazolium ring. In order to confirm whether chloride anion took part in the reaction, the CWPO of BmimCl, which was conducted with a IL concentration of 1 mM and the stoichiometric amount of H_2O_2 at 80 ºC at pH 3, was also performed by using 1 mM HNO_3 instead of HCl to adjust the pH of the medium. Chloride anion remained unchanged under the alternative conditions, and, unlike the electrolytic process, no chlorate or perchlorate ion was formed [55].

Apart from short-chain acids and nitrate anion, heteroaromatic and hydroxylated derivatives of 1-butyl-3-methylimidazolium oxidation were identified by LC–MS at different CWPO reaction times for BmimCl. Figure 4 depicts a potential reaction pathway for $Bmim^+$ in the CWPO reaction. The initial cation, with m/z = 139, may have undergone a hydroxyl radical attack on its side-chain or even oxidation of the imidazolium ring, as other authors suggest for imidazolium ILs in Fenton reaction [37,44]. The second step involves cleavage of the alkyl chain leading to the formation of different heteroaromatic compounds which are degraded to open-ring intermediates. Subsequent degradation of these compounds gives short-chain acids that are eventually converted into CO_2, H_2O and nitrate. Some of these intermediates were previously identified by other authors in the electrochemical degradation of imidazolium ILs. Siedlecka et al. (2013) and Pieczýnska et al. (2015) observed the m/z = 68, m/z = 82

and m/z = 154 species in the electroxidation of BmimCl [26,56] and Mena et al. (2017), besides the abovementioned compounds, detected the m/z = 73 and m/z = 102 ones in the BmimCl and BmimAc electroxidation [28]. Finally, reaction Gomez-Herrero et al. (2018) observed, as reaction intermediates of HmimCl by Fenton oxidation, the m/z = 73, m/z = 82 and m/z = 154 species [44].

One of the greatest advantages of ionic liquids is that they can be designed for specific purposes by using a suitable cation–anion combination. The composition of an IL can therefore influence its ease of degradation [24,35]. Table 3 shows the results obtained in the CWPO of BmimCl, BmimAc, and $BmimNTf_2$ at temperatures from 70 to 90 ºC. The apparent kinetic constants describing $Bmim^+$ disappearance during the reaction were calculated by assuming a pseudo first-order dependence on the $Bmim^+$ concentration. As expected, the constants increased with increasing reaction temperature; also, there were no significant differences among ILs in this respect. H_2O_2 conversion increased with increasing temperature and amounted to nearly 93 % at 90 ºC, again the nature of the anion seemingly having no influence on the extent of H_2O_2 decomposition in the CWPO process. Nor was the type of anion used influential on TOC conversion, the greatest difference among ILs being less than 5 %. However, raising the temperature increased TOC conversion up to 3 times with all ILs, as previously observed in the Fenton and CWPO reactions of various organic pollutants [46,53,57], and also in the Fenton reaction [37,42] and electrolysis [26] of diverse ILs. The proposed pathway for BmimCl is applicable to these ILs; therefore, after 240 min, the reaction medium will contain short-chain acids (acetic, oxalic and formic), nitrates and the same intermediates formed in BmimCl degradation. Table 3 includes an estimate of the carbon balance compliance ($C_{identified}$) at the end of each run as calculated as the ratio of concentrations of short-chain acids (C_{acids}) and anions (C_{anion}) in terms of carbon, and the total organic

carbon. The highest reaction temperature favored identification of total organic carbon. TOC was present in large amounts with the ILs containing organic anions (acetate or NTf_2^-), which are typically refractory to CWPO.

Table 3. Pseudo-first order constants and results after 240 min of CWPO of imidazolium ILs with Fe/γ-Al_2O_3 catalyst.

T (ºC)	IL	k_{Bmim} (min^{-1})	χ_{H2O2} (%)	χ_{TOC} (%)	ΣC_{acids} (mg L^{-1})	C_{anion} (mg L^{-1})	$C_{identified}$ (%)
70	BmimCl	$2.5 \cdot 10^{-2}$	73.2	7.3	7.9	–	8.9
	BmimAc	$1.8 \cdot 10^{-2}$	70.9	7.3	12.3	24.3	32.9
	$BmimNTf_2$	$2.0 \cdot 10^{-2}$	73.9	10.6	12.6	24.1	34.2
80	BmimCl	$5.2 \cdot 10^{-2}$	79.4	21.7	10.1	–	13.4
	BmimAc	$6.3 \cdot 10^{-2}$	80.5	24.8	14.2	23.9	42.2
	$BmimNTf_2$	$6.1 \cdot 10^{-2}$	82.0	26.2	14.8	24.2	44.0
90	BmimCl	$7.4 \cdot 10^{-2}$	91.2	42.7	11.8	–	21.5
	BmimAc	$8.0 \cdot 10^{-2}$	92.5	40.7	15.7	23.7	55.4
	$BmimNTf_2$	$7.5 \cdot 10^{-2}$	92.9	40.9	17.8	24.7	59.9

$[IL]_0$ = 1 mM, $[H_2O_2]_0$ = 27 mM, [Fe] = 40 mg L^{-1}, pH_0 = 3

The nature of the anion had virtually no effect on the CWPO reaction. NTf_2^- and Cl^- remained unchanged during the process; by contrast, acetate ion increased slightly in concentration, possibly by effect of its being recalcitrant to CWPO degradation and of its scant formation, together with other short-chain acids, in $Bmim^+$ degradation [58].

3.2. Influence of the alkyl chain

The length of the alkyl side chain has been related to the degradation rate and toxicity of ILs [7,59]. This led us to study imidazolium-based ILs with different *n*-alkyl chains (BmimCl, HmimCl and DmimCl) in the CWPO reaction at 70, 80 and 90 ºC. For the different temperatures assayed, all cations were completely degraded and no significant differences among the concentrations of $Bmim^+$, $Hmim^+$ and $Dmim^+$ versus reaction time for each temperature were observed (data not shown). Similar results were reported

for Fenton or heterogeneous Fenton reactions, where a slightly increase of reaction rate was only observed for imidazolium ILs with alkyl chain lengths of more than 12 carbons [39,41].

As regards mineralization, TOC conversion ranged from 40 to 50 % and was highest for DmimCl as a result of its increased carbon content. Also related to TOC conversion, the proportion of carbon in the compounds identified at 90 ºC differed slightly: from 21.5 % in BmimCl to 22.5 % in HmimCl to 26 % in DmimCl. The pseudo first-order kinetic constant for cation degradation ranged from $7.3 \cdot 10^{-2}$ to $7.5 \cdot 10^{-2}$ min^{-1} and, consistent with previous results, was not influenced by the length of the alkyl side chain [39,41]. In a previous electrochemical degradation experiment on imidazolium ILs, those with the longer alkyl side chains exhibited faster degradation, their kinetic constants as determined with a boron-doped diamond electrode being $1.97 \cdot 10^{-2}$ min^{-1} for BmimCl and $2.22 \cdot 10^{-2}$ min^{-1} for HmimCl [26]. Based on these results, CWPO is more efficient than electrolysis in degrading imidazolium-based ILs.

3.3. Biodegradability of the ionic liquids

Wastewater containing ILs is usually poorly biodegradable even though IL cations with a long side chain can be partially degraded [20,21]. This led us to conduct CWPO runs of imidazolium ILs to improve the biodegradability of this type of waste. Figure 5 shows the biodegradability of the initial and final effluent of ILs. Based on the results, BmimCl, $BmimNTf_2$, HmimCl and DmimCl are not readily biodegradable [4,60,61]; in fact, no changes in cation or TOC concentration, nor significant variations in SOUR, were detected in the biodegradability tests. However, the fact that endogenous respiration (ca. 3–4 mg O_2 g_{SV}^{-1} h^{-1}) was constant suggests that the poor biodegradability of the ILs was not associated to a high toxicity. Changes in SOUR and

IL concentration exhibited a differential pattern for BmimAc; thus, SOUR increased and TOC proportionally decreased over the first few hours of reaction. The decrease in TOC was a result of degradation of acetate anion with no change in $Bmim^+$ concentration. As with the other ILs, SOUR and TOC levelled off after 5 h. The CWPO effluents for each IL treated were subjected to the same test. In all cases, SOUR increased by effect of the decomposition of easily degraded species formed in the CWPO reaction (e.g., acetate ion). A second increase in SOUR occurred between 20 and 40 h of reaction in the BmimCl and BmimAc effluents concomitantly with a decrease in TOC due to degradation of some reaction intermediates that required pre-acclimation to the activated sludge. Some authors have suggested that the short-chain acids oxalic and formic, which are typically involved in Fenton and CWPO reactions, can be degraded by conventional biological treatment [52,53]. In fact, both were easily removed from the effluents within 50 h. No second SOUR increase was observed with $BmimNTf_2$. However, a slightly decreased endogenous respiration was observed in the activated sludge between 30 and 70 h as a result of a decrease in microbial population. This result may have arisen from the formation of toxic intermediates in the CWPO reaction. As regards TOC degradation, the biodegradability assay revealed a decrease in TOC by 35 % in the BmimCl and $BmimNTf_2$ effluents, and one of 40 % in the BmimAc effluent. Combining CWPO and the biodegradability assay led to a total TOC conversion level roughly 55–60 % higher than that achieved by CWPO at 90 ºC (ca. 40 %), which was the highest temperature studied. The high toxicity of HmimCl and DmimCl, required carrying out the CWPO reactions at the maximum possible temperature, which ensures a greater transformation of the starting compound. The effluents present a first SOUR increased in the first hours as the Bmim-ILs, and a second increased at 40 h wider than the Bmim-IL ones.

The *Daphnia* toxicity test was used to assess the effect of CWPO on the IL solutions. As can be seen in the Table 4 the EC_{50} values for BmimCl and BmimAc were similar but greater than that for $BmimNTf_2$. Also, toxicity increased with increasing length of the alkyl side chain [7,17,62]; thus, DmimCl toxicity was more than 300 times higher than BmimCl toxicity. Ecotoxicity values upon CWPO exhibited two different trends. The Bmim-based ILs became more toxic through the production of more toxic intermediates than the initial ILs, toxicity increasing in the sequence BmimCl < BmimAc < $BmimNTf_2$. Also, BmimCl toxicity decreased with increasing CWPO temperature as a result of the intermediates being converted into less toxic species. By contrast, the ILs with the longest alkyl side chains were much less toxic after CWPO, but their effluents were still more toxic than those of BmimCl.

Table 4. Results of the *Daphnia* assay for the initial and final CWPO effluents.

	Initial solution		**CWPO effluent, 80 ºC**	**CWPO effluent, 90 ºC**
IL	**Log EC_{50}**	**EC_{50} (mM)**	**log IC_{50}**	**log IC_{50}**
BmimCl	2.017 ± 0.041	104.1	1.637 ± 0.060	1.799 ± 0.068
BmimAc	2.000 ± 0.016	100.0	1.383 ± 0.050	–
$BmimNTf_2$	1.913 ± 0.077	81.9	1.291 ± 0.028	–
HmimCl	1.090 ± 0.056	12.8	–	1.679 ± 0.031
DmimCl	–0.530 ± 0.168	0.29	–	1.401 ± 0.029

3.4. Catalyst stability

A long-term experiment was carried out to assess the stability of the catalyst in the CWPO reaction with a view to removing ILs from wastewater. The experiment was performed with BmimAc because it had previously exhibited high mineralization in the combined process (CWPO + biodegradability assay). Figure 6 shows the variation of the $Bmim^+$ cation and also TOC and H_2O_2 conversion at 3.33 $kg_{Fe2O3/Al2O3}$ h mol_{IL}^{-1}. The $Bmim^+$ concentration rapidly decreased from 1.0 to 0.4 mM and then remained at that

level for more than 75 h. The cation transformation resulted in an increase in the initial acetate concentration by 0.1 mM by effect of the formation of acetic acid. TOC and H_2O_2 conversion gradually increased while the system stabilized and eventually leveled off at 18 % and 30 %, respectively. In terms of short-chain acids, acetic and formic were detected at a concentration of 1.1 and 0.2 mM, respectively, and oxalic at a much lower level (0.02 mM). Based on the proposed reaction pathway for $Bmim^+$, the reaction medium contained heteroaromatic compounds with an equivalent carbon concentration of 4.5 mM of unidentified TOC.

The properties of the used catalyst were compared with those of the fresh catalyst in Table 2. The used catalyst exhibited no significant difference in pore structure (A_{BET} = 120 m^2 g^{-1}; $V_{mesopores}$ = 0.110 cm^3 g^{-1}). As regards Fe leaching, which is the most plausible cause of catalyst deactivation in CWPO reactions [53,63–65], TXRF analysis revealed little loss of Fe during the reaction on stream, the total amount of Fe in the used catalyst (3.86 % w/w) being quite similar to that in the fresh catalyst. Fe_{XPS} was identical in the fresh and used catalyst, which can therefore be deemed stable in the CWPO of ILs. Elemental analyses revealed slight deposition of residual carbon (2.5 % w/w) on the catalyst surface which seemingly caused no blockage of active sites. The consistency of IL and TOC conversion in the process is correlated with the stability in the catalyst properties.

4. Conclusions

Catalytic wet peroxidation (CWPO) in the presence of a Fe_2O_3/Al_2O_3 catalyst proved an effective treatment for the removal of imidazolium ILs (BmimCl, BmimAc, $BmimNTf_2$, HmimCl and DmimCl) from wastewater. Thus, $Bmim^+$ cation was completely removed after 240 min at 80 ºC with similar efficiency (0.033 mg_{TOC} mg_{H2O2}^{-1}) irrespective of

the H_2O_2 dose used. The highest mineralization rate was obtained by using the stoichiometric amount of H_2O_2 at 90 ºC (40%). In terms of anions, the acetate concentration increased along reaction time, due to its refractory behavior in CWPO reactions, whereas chloride and NTf_2^- concentration remained unalterable. Mineralization increased with increasing length of the alkyl side chain, but the extent of imidazolium cation removal was essentially the same. The Fe_2O_3/Al_2O_3 catalyst showed a fairly low Fe leaching, below 0.05 mg L^{-1} in all cases. A degradation pathway involving heteroaromatic and hydroxylated derivatives of $Bmim^+$ cation, short-chain acids and nitrate detected at the end of the reaction (240 min) is proposed. CWPO increased biodegradability in the final effluents relative to the initial ones and TOC conversion after CWPO-biodegradability process being 55–60 %. The Fe_2O_3/Al_2O_3 catalyst used exhibited long-term stability along CWPO of BmimAc (3.33 $kg_{Fe2O3/Al2O3}$ h mol_{IL}^{-1}); thus, it remained stable for 70 h in an on-stream experiment lasting 100 h. The used catalyst had essentially the same Fe content as the starting catalyst, which confirms the absence of Fe leaching.

Acknowledgments

The authors acknowledge funding from Spain's MINECO (CTM2016-76564-R), the Madrid Regional Government (S2013/MAE-2716), UAM-Santander (CEAL-AL/2015-08) and UNAM Engineering Institute (II-4307). I. F. Mena also thanks MINECO and ESF for award of a research grant.

References

[1] S. Stolte, S. Steudte, O. Areitioaurtena, F. Pagano, J. Thöming, P. Stepnowski, et

al., Ionic liquids as lubricants or lubrication additives: An ecotoxicity and biodegradability assessment, Chemosphere. 89 (2012) 1135–1141. doi:10.1016/j.chemosphere.2012.05.102.

[2] M. Markiewicz, M. Piszora, N. Caicedo, C. Jungnickel, S. Stolte, Toxicity of ionic liquid cations and anions towards activated sewage sludge organisms from different sources -- consequences for biodegradation testing and wastewater treatment plant operation., Water Res. 47 (2013) 2921–8. doi:10.1016/j.watres.2013.02.055.

[3] J. Neumann, M. Pawlik, D. Bryniok, J. Thöming, S. Stolte, Biodegradation potential of cyano-based ionic liquid anions in a culture of Cupriavidus spp. and their in vitro enzymatic hydrolysis by nitrile hydratase, Environ. Sci. Pollut. Res. 21 (2014) 9495–9505. doi:10.1007/s11356-013-2341-2.

[4] A. Romero, A. Santos, J. Tojo, A. Rodriguez, Toxicity and biodegradability of imidazolium ionic liquids, J. Hazard. Mater. 151 (2008) 268–273. doi:10.1016/j.jhazmat.2007.10.079.

[5] C. Abrusci, J. Palomar, J.L. Pablos, F. Rodriguez, F. Catalina, Efficient biodegradation of common ionic liquids by Sphingomonas paucimobilis bacterium, Green Chem. 13 (2011) 709–717. doi:10.1039/c0gc00766h.

[6] R. Biczak, B. Pawlowska, P. Balczewski, P. Rychter, The role of the anion in the toxicity of imidazolium ionic liquids, J. Hazard. Mater. 274 (2014) 181–190. doi:10.1016/j.jhazmat.2014.03.021.

[7] H. Liu, X. Zhang, C. Chen, S. Du, Y. Dong, Effects of imidazolium chloride ionic liquids and their toxicity to Scenedesmus obliquus, Ecotoxicol. Environ. Saf. 122 (2015) 83–90. doi:10.1016/j.ecoenv.2015.07.010.

[8] S.P.M. Ventura, C.S. Marques, A.A. Rosatella, C.A.M. Afonso, F. Gonçalves,

J.A.P. Coutinho, Toxicity assessment of various ionic liquid families towards Vibrio fischeri marine bacteria, Ecotoxicol. Environ. Saf. 76 (2012) 162–168. doi:10.1016/j.ecoenv.2011.10.006.

[9] A. Jordan, N. Gathergood, Biodegradation of ionic liquids - a critical review., Chem. Soc. Rev. 44 (2015) 8200–8237. doi:10.1039/c5cs00444f.

[10] A. Santiago, R. Castillo, S. Guihéneuf, R. Le, Synthesis and toxicity evaluation of hydrophobic ionic liquids for volatile organic compounds biodegradation in a two-phase partitioning bioreactor, J. Hazard. Mater. 307 (2016) 221–230. doi:10.1016/j.jhazmat.2015.12.043.

[11] R.L. Vekariya, A review of ionic liquids: Applications towards catalytic organic transformations, J. Mol. Liq. 227 (2017) 44–60. doi:10.1016/j.molliq.2016.11.123.

[12] C.W. Cho, Y.C. Jeon, T.P.T. Pham, K. Vijayaraghavan, Y.S. Yun, The ecotoxicity of ionic liquids and traditional organic solvents on microalga Selenastrum capricornutum, Ecotoxicol. Environ. Saf. 71 (2008) 166–171. doi:10.1016/j.ecoenv.2007.07.001.

[13] M. Amde, J. Liu, L. Pang, Environmental Application , Fate , Effects and Concerns of Ionic Liquids : A Review, (2015). doi:10.1021/acs.est.5b03123.

[14] S.P.F. Costa, P.C.A.G. Pinto, M.L.M.F.S. Saraiva, F.R.P. Rocha, J.R.P. Santos, R.T.R. Monteiro, The aquatic impact of ionic liquids on freshwater organisms, Chemosphere. 139 (2015) 288–294. doi:10.1016/j.chemosphere.2015.05.100.

[15] F.J. Hernández-Fernández, J. Bayo, A. Pérez de los Ríos, M.A. Vicente, F.J. Bernal, J. Quesada-Medina, Discovering less toxic ionic liquids by using the Microtox® toxicity test, Ecotoxicol. Environ. Saf. 116 (2015) 29–33. doi:10.1016/j.ecoenv.2015.02.034.

[16] M.I. Khan, D. Zaini, A.M. Shariff, Framework for Ecotoxicological Risk Assessment of Ionic Liquids, Procedia Eng. 148 (2016) 1141–1148. doi:10.1016/j.proeng.2016.06.567.

[17] T.P. Thuy Pham, C.W. Cho, Y.S. Yun, Environmental fate and toxicity of ionic liquids: A review, Water Res. 44 (2010) 352–372. doi:10.1016/j.watres.2009.09.030.

[18] S.P.M. Ventura, F.A. e Silva, A.M.M. Gonçalves, J.L. Pereira, F. Gonçalves, J.A.P. Coutinho, Ecotoxicity analysis of cholinium-based ionic liquids to Vibrio fischeri marine bacteria, Ecotoxicol. Environ. Saf. 102 (2014) 48–54. doi:10.1016/j.ecoenv.2014.01.003.

[19] S.P.F. Costa, P.C.A.G. Pinto, R.A.S. Lapa, M.L.M.F.S. Saraiva, Toxicity assessment of ionic liquids with Vibrio fischeri: An alternative fully automated methodology, J. Hazard. Mater. 284 (2014) 136–142. doi:10.1016/j.jhazmat.2014.10.049.

[20] K.M. Docherty, J.K. Dixon, C.F. Kulpa, Biodegradability of imidazolium and pyridinium ionic liquids by an activated sludge microbial community, Biodegradation. 18 (2007) 481–493. doi:10.1007/s10532-006-9081-7.

[21] S. Stolte, S. Abdulkarim, J. Arning, A.K. Blomeyer-Nienstedt, U. Bottin-Weber, M. Matzke, et al., Primary biodegradation of ionic liquid cations, identification of degradation products of 1-methyl-3-octylimidazolium chloride and electrochemical wastewater treatment of poorly biodegradable compounds, Green Chem. 10 (2008) 214–224. doi:10.1039/b713095c.

[22] E. Neyens, J. Baeyens, A review of classic Fenton's peroxidation as an advanced oxidation technique, J. Hazard. Mater. 98 (2003) 33–50. doi:10.1016/S0304-3894(02)00282-0.

[23] J.J. Pignatello, E. Oliveros, A. MacKay, Advanced Oxidation Processes for Organic Contaminant Destruction Based on the Fenton Reaction and Related Chemistry, Crit. Rev. Environ. Sci. Technol. 36 (2006) 1–84. doi:10.1080/10643380500326564.

[24] A. Fabiańska, T. Ossowski, P. Stepnowski, S. Stolte, J. Thöming, E.M. Siedlecka, Electrochemical oxidation of imidazolium-based ionic liquids: The influence of anions, Chem. Eng. J. 198-199 (2012) 338–345. doi:10.1016/j.cej.2012.05.108.

[25] E.M. Siedlecka, S. Stolte, M. Golebiowski, A. Nienstedt, P. Stepnowski, J. Thöming, Advanced oxidation process for the removal of ionic liquids from water: The influence of functionalized side chains on the electrochemical degradability of imidazolium cations, Sep. Purif. Technol. 101 (2012) 26–33. doi:10.1016/j.seppur.2012.09.012.

[26] A. Pieczyńska, A. Ofiarska, A.F. Borzyszkowska, A. Białk-Bielińska, P. Stepnowski, S. Stolte, et al., A comparative study of electrochemical degradation of imidazolium and pyridinium ionic liquids: A reaction pathway and ecotoxicity evaluation, Sep. Purif. Technol. 156 (2015) 522–534. doi:10.1016/j.seppur.2015.10.045.

[27] S. Garcia-Segura, Á.S. Lima, E.B. Cavalcanti, E. Brillas, Anodic oxidation, electro-Fenton and photoelectro-Fenton degradations of pyridinium- and imidazolium-based ionic liquids in waters using a BDD/air-diffusion cell, Electrochim. Acta. 198 (2016) 268–279. doi:10.1016/j.electacta.2016.03.057.

[28] I.F. Mena, S. Cotillas, E. Díaz, C. Sáez, Á.F. Mohedano, M.A. Rodrigo, Sono- and photoelectrocatalytic processes for the removal of ionic liquids based on the 1-butyl-3-methylimidazolium cation, J. Hazard. Mater. (2017) 1–8.

doi:10.1016/j.jhazmat.2017.12.015.

[29] I.F. Mena, S. Cotillas, E. Díaz, C. Sáez, J.J. Rodríguez, P. Cañizares, et al., Electrolysis with diamond anodes: Eventually, there are refractory species!, Chemosphere. 195 (2018) 771–776. doi:10.1016/j.chemosphere.2017.12.120.

[30] I.F. Mena, S. Cotillas, E. Díaz, C. Sáez, Á.F. Mohedano, M.A. Rodrigo, Influence of the supporting electrolyte on the removal of ionic liquids by electrolysis with diamond anodes, Catal. Today. (2017) 0–1. doi:10.1016/j.cattod.2017.10.025.

[31] P. Stepnowski, A. Zaleska, Comparison of different advanced oxidation processes for the degradation of room temperature ionic liquids, J. Photochem. Photobiol. A Chem. 170 (2005) 45–50. doi:10.1016/j.jphotochem.2004.07.019.

[32] M. Czerwicka, S. Stolte, A. Müller, E.M. Siedlecka, M. Gołebiowski, J. Kumirska, et al., Identification of ionic liquid breakdown products in an advanced oxidation system, J. Hazard. Mater. 171 (2009) 478–483. doi:10.1016/j.jhazmat.2009.06.027.

[33] D. Spasiano, A. Siciliano, M. Race, R. Marotta, M. Guida, R. Andreozzi, et al., Biodegradation, ecotoxicity and UV254/H2O2 treatment of imidazole, 1-methyl-imidazole and N,N'-alkyl-imidazolium chlorides in water, Water Res. 106 (2016) 450–460. doi:10.1016/j.watres.2016.10.026.

[34] E.M. Siedlecka, W. Mrozik, Z. Kaczyński, P. Stepnowski, Degradation of 1-butyl-3-methylimidazolium chloride ionic liquid in a Fenton-like system, J. Hazard. Mater. 154 (2008) 893–900. doi:10.1016/j.jhazmat.2007.10.104.

[35] E.M. Siedlecka, M. Gołebiowski, Z. Kaczyński, J. Czupryniak, T. Ossowski, P. Stepnowski, Degradation of ionic liquids by Fenton reaction; the effect of anions as counter and background ions, Appl. Catal. B Environ. 91 (2009) 573–579.

doi:10.1016/j.apcatb.2009.06.029.

[36] M. Munoz, C.M. Domínguez, Z.M. De Pedro, A. Quintanilla, J.A. Casas, S.P.M. Ventura, et al., Role of the chemical structure of ionic liquids in their ecotoxicity and reactivity towards Fenton oxidation, Sep. Purif. Technol. 150 (2015) 252–256. doi:10.1016/j.seppur.2015.07.014.

[37] M. Munoz, C.M. Dominguez, Z.M. De Pedro, A. Quintanilla, J.A. Casas, J.J. Rodriguez, Ionic liquids breakdown by Fenton oxidation, Catal. Today. 240 (2015) 16–21. doi:10.1016/j.cattod.2014.03.028.

[38] F. Chen, S. Xie, X. Huang, X. Qiu, Ionothermal synthesis of Fe3O4 magnetic nanoparticles as efficient heterogeneous Fenton-like catalysts for degradation of organic pollutants with H2O2, J. Hazard. Mater. 322 (2017) 152–162. doi:10.1016/j.jhazmat.2016.02.073.

[39] M. Munoz, C.M. Domínguez, Z.M. de Pedro, A. Quintanilla, J.A. Casas, J.J. Rodriguez, Degradation of imidazolium-based ionic liquids by catalytic wet peroxide oxidation with carbon and magnetic iron catalysts, J. Chem. Technol. Biotechnol. 91 (2016) 2882–2887. doi:10.1002/jctb.4904.

[40] V. Pazo-Nogueira, M. Arellano, E. Rosales, M. Pazos, E. González-Romero, M.A. Sanromán, Heterogeneous electro-Fenton as plausible technology for the degradation of imidazolinium-based ionic liquids, Chemosphere. 199 (2018) 68–75. doi:10.1016/j.chemosphere.2018.01.174.

[41] C.M. Domínguez, M. Munoz, A. Quintanilla, M. De Pedro, S.P.M. Ventura, J.A.P. Coutinho, et al., Degradation of imidazolium-based ionic liquids in aqueous solution by Fenton oxidation, J Chem Technol Biotechnol. 89 (2014) 1197 – 1202. doi:10.1002/jctb.4366.

[42] H. Cheng, G. Chen, Y. Qiu, B. Li, M.K. Stenstrom, Factors that influence the

degradation of 1-ethyl-3- methylimidazolium hexafluorophosphate by Fenton oxidation, R. Soc. Chem. 6 (2016) 59889–59895. doi:10.1039/C6RA12675H.

[43] C.M. Domínguez, M. Munoz, A. Quintanilla, Z.M. de Pedro, J.A. Casas, Kinetics of imidazolium-based ionic liquids degradation in aqueous solution by Fenton oxidation, Environ. Sci. Pollut. Res. (2017). doi:10.1007/s11356-017-0459-3.

[44] E. Gomez-Herrero, M. Tobajas, A. Polo, J.J. Rodriguez, A.F. Mohedano, Removal of imidazolium- and pyridinium-based ionic liquids by Fenton oxidation, Environ. Sci. Pollut. Res. (2018). doi:10.1007/s11356-017-0867-4.

[45] E. Bocos, M. Pazos, M.Á. Sanromán, Electro-Fenton treatment of imidazolium-based ionic liquids: Kinetics and degradation pathways, RSC Adv. 6 (2016) 1958–1965. doi:10.1039/c5ra24070k.

[46] P. Bautista, A.F. Mohedano, J.A. Casas, J.A. Zazo, J.J. Rodriguez, Highly stable Fe/γ-Al2O3 catalyst for catalytic wet peroxide oxidation, J. Chem. Technol. Biotechnol. 86 (2011) 497–504. doi:10.1002/jctb.2538.

[47] A. Rey, A.B. Hungria, C.J. Duran-valle, M. Faraldos, A. Bahamonde, J.A. Casas, et al., On the optimization of activated carbon-supported iron catalysts in catalytic wet peroxide oxidation process, Appl. Catal. B, Environ. 181 (2016) 249–259. doi:10.1016/j.apcatb.2015.07.051.

[48] J. Bedia, V.M. Monsalvo, J.J. Rodriguez, A.F. Mohedano, Iron catalysts by chemical activation of sewage sludge with FeCl 3 for CWPO, Chem. Eng. J. (2016). doi:10.1016/j.cej.2016.06.096.

[49] G. Eisenberg, Colorimetric Determination of Hydrogen Peroxide, Nd. Eng. Chem. Anal. Ed. 15 (1943) 327–328.

[50] E.B. Sandell, Determination of Traces of Metals, third ed., Interscience Pubs, New York, NY, 1959.

[51] A.M. Polo, M. Tobajas, S. Sanchis, A.F. Mohedano, J.J. Rodriguez, Comparison of experimental methods for determination of toxicity and biodegradability of xenobiotic compounds, Biodegradation. 22 (2011) 751–761. doi:10.1007/s10532-010-9448-7.

[52] V.M. Monsalvo, J. Lopez, M. Munoz, Z.M. de Pedro, J.A. Casas, A.F. Mohedano, et al., Application of Fenton-like oxidation as pre-treatment for carbamazepine biodegradation, Chem. Eng. J. 264 (2015) 856–862. doi:10.1016/j.cej.2014.11.141.

[53] I.F. Mena, E. Diaz, J.J. Rodriguez, A.F. Mohedano, CWPO of bisphenol A with iron catalysts supported on microporous carbons from grape seeds activation, Chem. Eng. J. 318 (2016) 153–160. doi:10.1016/j.cej.2016.06.029.

[54] P. Bautista, A.F. Mohedano, N. Menéndez, J.A. Casas, J.J. Rodriguez, Catalytic wet peroxide oxidation of cosmetic wastewaters with Fe-bearing catalysts, Catal. Today. 151 (2010) 148–152. doi:10.1016/j.cattod.2010.01.023.

[55] S. Neodo, D. Rosestolato, S. Ferro, A. De Battisti, On the electrolysis of dilute chloride solutions: Influence of the electrode material on Faradaic efficiency for active chlorine, chlorate and perchlorate, Electrochim. Acta. 80 (2012) 282–291. doi:10.1016/j.electacta.2012.07.017.

[56] E.M. Siedlecka, A. Fabiañska, S. Stolte, A. Nienstedt, T. Ossowski, P. Stepnowski, et al., Electrocatalytic oxidation of 1-butyl-3-methylimidazolium chloride: Effect of the electrode material, Int. J. Electrochem. Sci. 8 (2013) 5560–5574.

[57] N. Inchaurrondo, J. Cechini, J. Font, P. Haure, Strategies for enhanced CWPO of phenol solutions, Appl. Catal. B Environ. 111-112 (2012) 641–648. doi:10.1016/j.apcatb.2011.11.019.

[58] G. Centi, S. Perathoner, T. Torre, M.G. Verduna, Catalytic wet oxidation with H2O2 of carboxylic acids on homogeneous and heterogeneous Fenton-type catalysts, Catal. Today. 55 (2000) 61–69. doi:10.1016/S0920-5861(99)00226-6.

[59] J. Ranke, K. Mölter, F. Stock, U. Bottin-Weber, J. Poczobutt, J. Hoffmann, et al., Biological effects of imidazolium ionic liquids with varying chain lengths in acute Vibrio fischeri and WST-1 cell viability assays, Ecotoxicol. Environ. Saf. 58 (2004) 396–404. doi:10.1016/S0147-6513(03)00105-2.

[60] M.T. Garcia, N. Gathergood, P.J. Scammells, Biodegradable ionic liquids - Part II. Effect of the anion and toxicology, Green Chem. 7 (2005) 9–14. doi:Doi 10.1039/B411922c.

[61] G. Quijano, A. Couvert, A. Amrane, G. Darracq, C. Couriol, P. Le Cloirec, et al., Toxicity and biodegradability of ionic liquids: New perspectives towards whole-cell biotechnological applications, Chem. Eng. J. 174 (2011) 27–32. doi:10.1016/j.cej.2011.07.055.

[62] E. Diaz, V.M. Monsalvo, J. Lopez, I.F. Mena, J. Palomar, J.J. Rodriguez, et al., Assessment the ecotoxicity and inhibition of imidazolium ionic liquids by respiration inhibition assays, Ecotoxicol. Environ. Saf. 162 (2018) 29–34. doi:10.1016/j.ecoenv.2018.06.057.

[63] M. Munoz, Z.M. de Pedro, N. Menendez, J.A. Casas, J.J. Rodriguez, A ferromagnetic γ-alumina-supported iron catalyst for CWPO. Application to chlorophenols, Appl. Catal. B Environ. 136-137 (2013) 218–224. doi:10.1016/j.apcatb.2013.02.002.

[64] A.F. Mohedano, V.M. Monsalvo, J. Bedia, J. Lopez, J.J. Rodriguez, Highly stable iron catalysts from sewage sludge for CWPO, J. Environ. Chem. Eng. 2 (2014) 2359–2364. doi:10.1016/j.jece.2014.01.021.

[65] J. Bedia, V.M. Monsalvo, J.J. Rodriguez, A.F. Mohedano, Iron catalysts by chemical activation of sewage sludge with FeCl3 for CWPO, Chem. Eng. J. 318 (2017) 224–230. doi:10.1016/j.cej.2016.06.096.

Figure captions

Figure 1. Time course of $Bmim^+$ concentration (black symbols), H_2O_2 conversion (open symbols) and TOC conversion (grey symbols) in the CWPO (circles) and Fenton oxidation (triangles) of BmimCl with a stoichiometric dose of H_2O_2 at 80 ºC. $[Fe_2O_3/Al_2O_3]_0$ = 1 g L^{-1}, pH_0 = 3. Insert: Fe leaching in CWPO reaction.

Figure 2. (a) Time course of $Bmim^+$ concentration (black symbols), H_2O_2 conversion (open symbols) and TOC conversion (grey symbols) and (b) Fe leaching in the CWPO of BmimCl with 0.5 (triangles), 1 (circles) and 1.5 (squares) times the stoichiometric dose of H_2O_2 at 80 ºC. $[Fe_2O_3/Al_2O_3]_0$ = 1 g L^{-1}, pH_0 = 3.

Figure 3. Time course of short-chain acids identified in the CWPO of BmimCl with different H_2O_2 doses at 80 ºC. $[Fe_2O_3/Al_2O_3]_0$ = 1 g L^{-1}, pH_0 = 3.

Figure 4. Reaction pathway for the CWPO of $Bmim^+$ cation with the stoichiometric dose of H_2O_2 at 80 ºC. $[Fe_2O_3/Al_2O_3]_0$ = 1 g L^{-1}, pH_0 = 3.

Figure 5. Time course of TOC (triangles) and SOUR (squares) of the initial (1 mM, open symbols) and final effluents (solid symbols) in the CWPO of BmimCl, BmimAc and $BmimNTf_2$ at T = 80 ºC, HmimCl and DmimCl at T = 90 ºC, $[H_2O_2]_0$ = stoichiometric dose, $[Fe_2O_3/Al_2O_3]_0$ = 1 g $L^{-1}$and pH_0 = 3. Operating conditions for the biodegradability assay: 350 mg L^{-1} VSS, T = 25 ºC, t = 100 h.

Figure 6. Evolution of $Bmim^+$ concentration and TOC and H_2O_2 conversion in long-term performance of the Fe_2O_3/Al_2O_3catalyst upon CWPO of BmimAc at 80 ºC . [BmimAc] = 1 mM, $[H_2O_2]$ = stoichiometric dose, pH_0 = 3, τ = 3.33 $kg_{Fe2O3/Al2O3}$ h mol^{-1}_{IL}.

Figure 1.

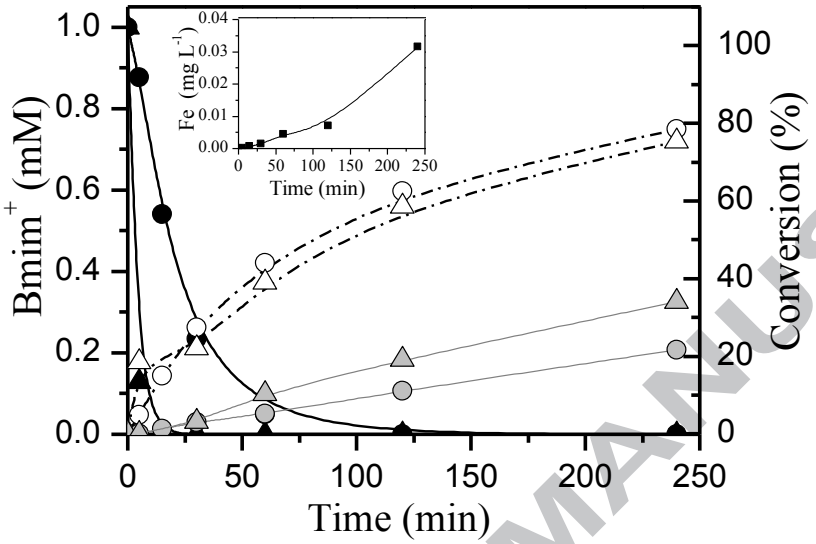

Figure 2.

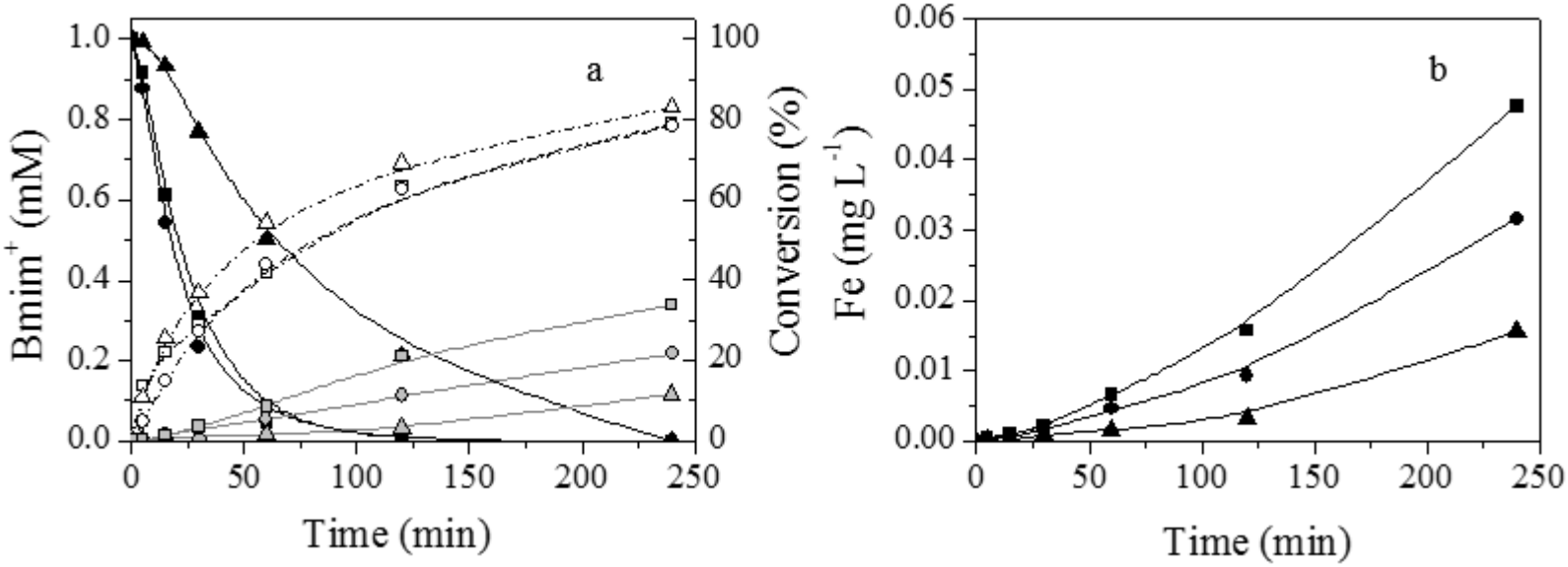

Figure 3.

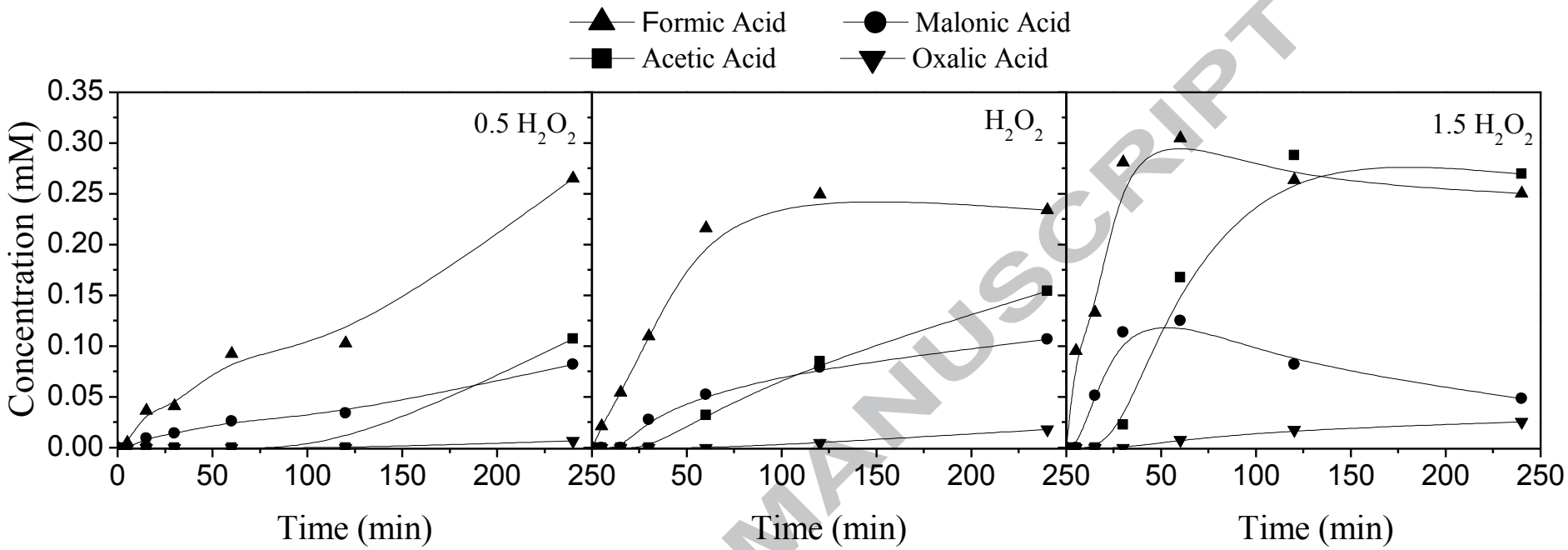

Figure 4.

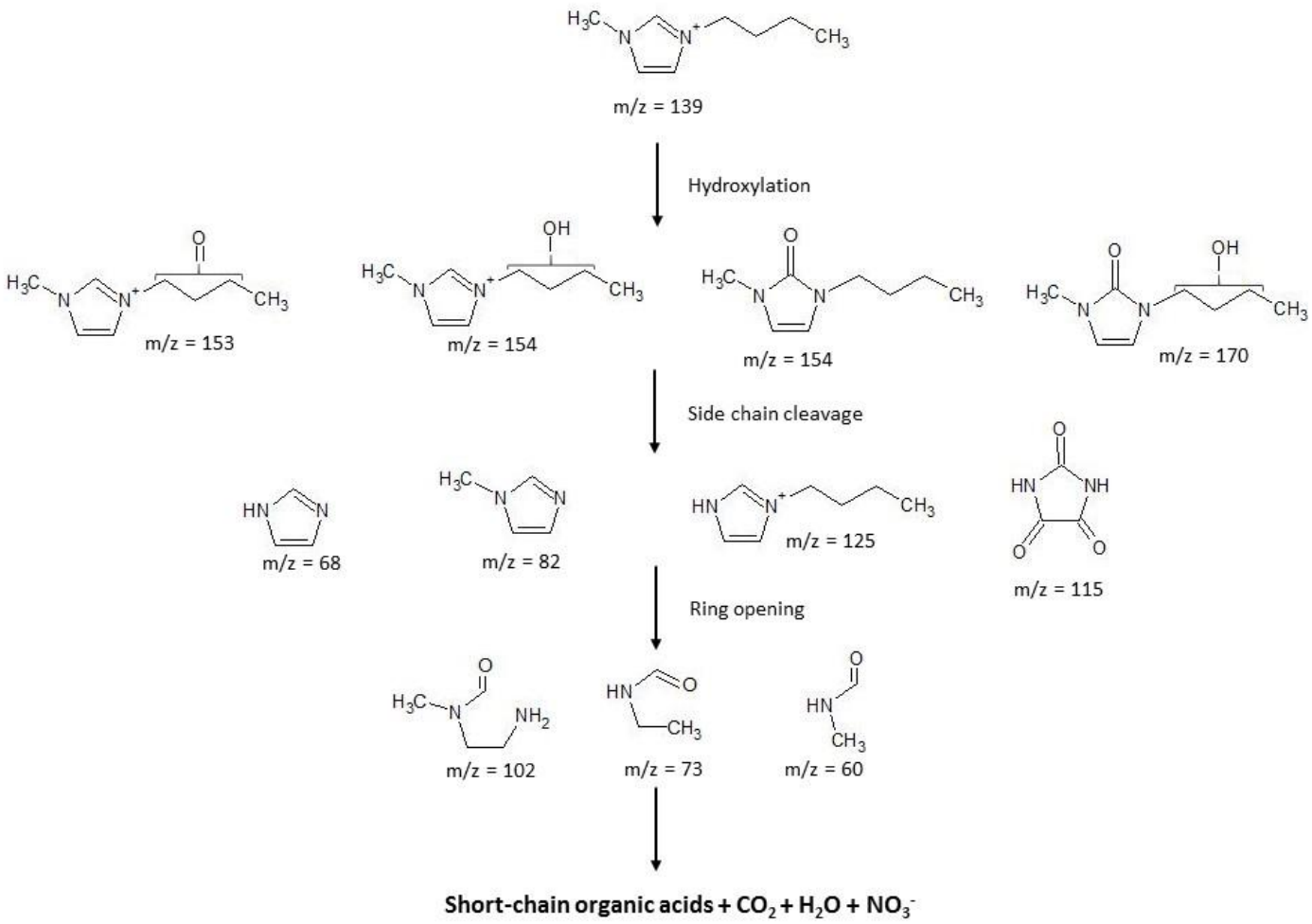

Figure 5.

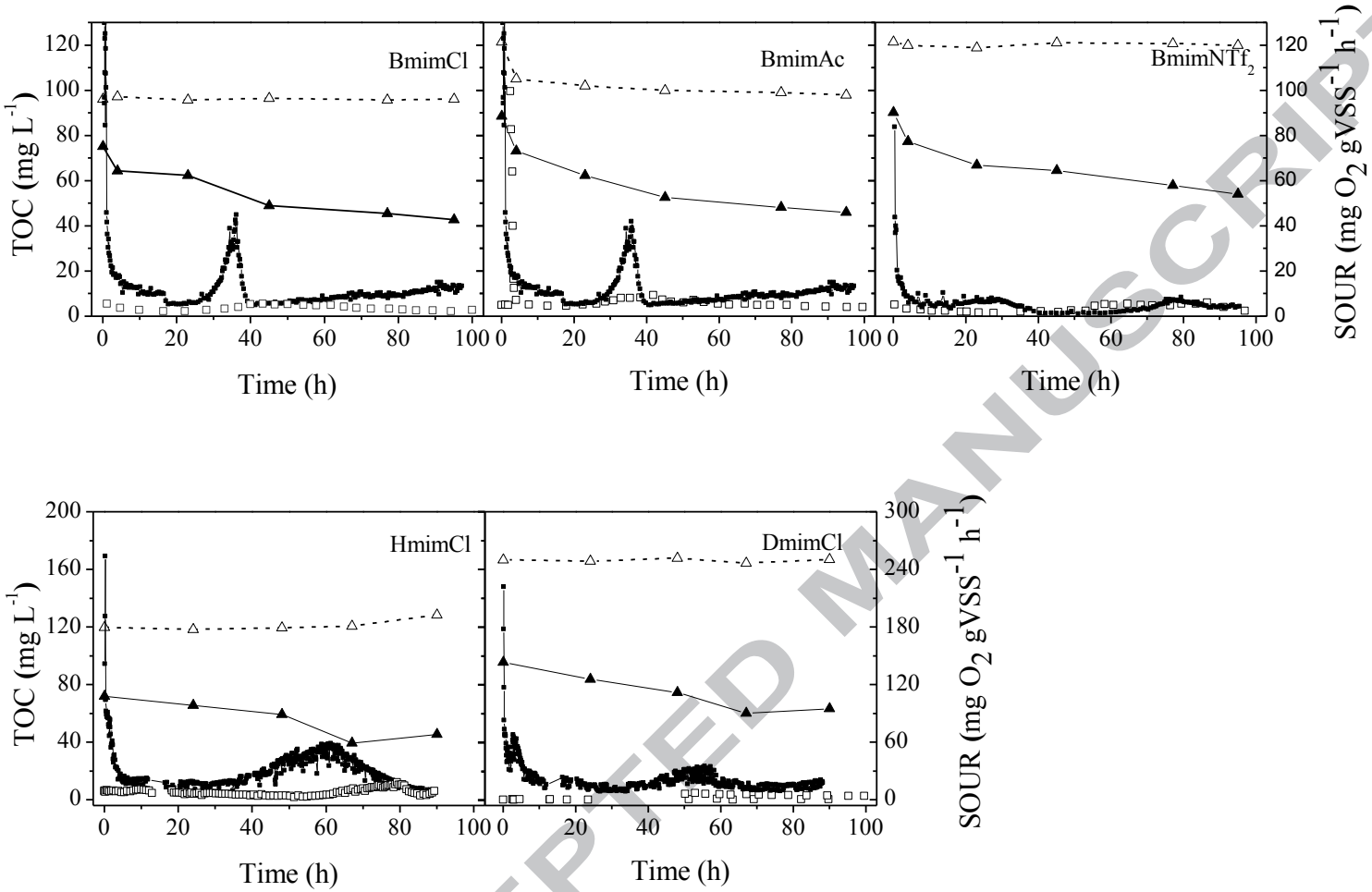

Figure 6.

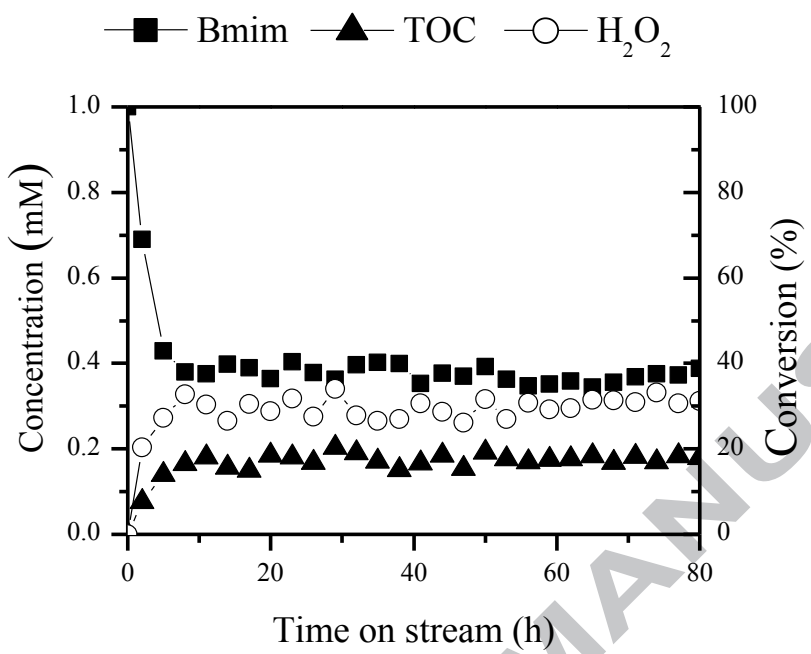

Graphical abstract

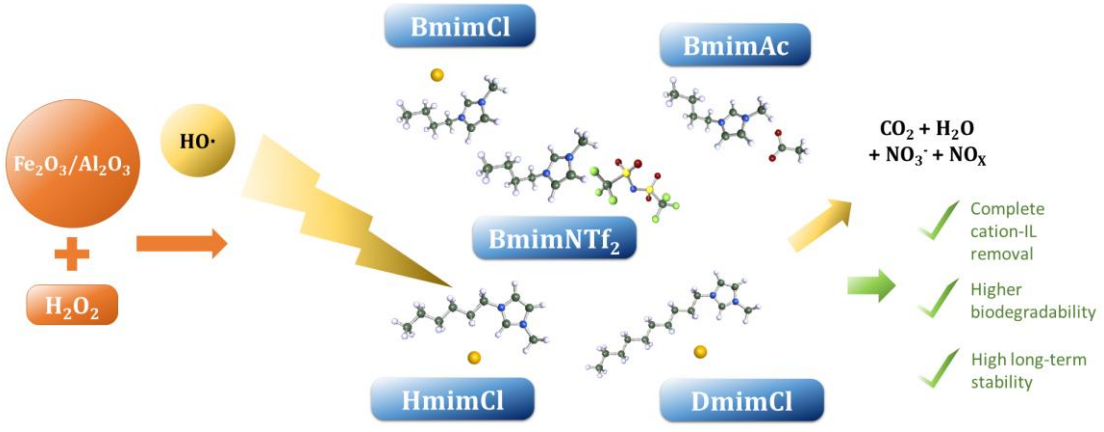

Highlights

- Fe/Al_2O_3 catalyst was highly active in the CWPO of imidazolium ionic liquids.
- Complete cation-IL removal was reached in CWPO reactions.
- Chloride, acetate and NTf_2 anions remained inalterable in the CWPO process.
- CWPO of ILs enhanced the biodegradability of the effluents.
- Fe/Al_2O_3 catalyst showed a high stability along 80 h time on stream.